NOAA TM EDS NODC-1

A UNI
DEPAR
COM
PUBL

NOAA Technical Memorandum EDS NODC

U.S. DEPARTMENT OF COMMERCE
National Oceanic and Atmospheric Administration
Environmental Data Service

Literature Search for Atmospheric Humidity Profile Models From the Sea Surface to 1,000 Meters

KENNETH R. AVERY

National
Oceanographic
Data Center

SILVER SPRING, MD.
February 1972

NOAA TECHNICAL MEMORANDA

EDS National Oceanographic Data Center Subseries

The National Oceanographic Data Center (NODC) of NOAA's Environmental Data Service (EDS) is the central United States repository for unclassified oceanographic data and related marine science information pertaining to the world's oceans, seas, and estuaries. The Center receives data and published information from both domestic and foreign sources, including national data centers of other countries and World Data Center A, Oceanography--the United States subcenter for oceanography in the World Data Center system. NODC compiles the National Marine Data Inventory, which contains information on quantities and types of data, areas of operations, and responsible personnel. NODC services include data processing, reproduction of data, preparation of data summaries and inventories, evaluation of data records, special literature searches, and provision of general marine sciences information.

NOAA Technical Memoranda in the EDS NODC subseries facilitate rapid dissemination of information that may be preliminary in nature and subject to formal publication elsewhere at a later date.

U.S. DEPARTMENT OF COMMERCE
National Oceanic and Atmospheric Administration
Environmental Data Service

NOAA Technical Memorandum EDS NODC-1

LITERATURE SEARCH FOR ATMOSPHERIC HUMIDITY PROFILE MODELS FROM THE SEA SURFACE TO 1,000 METERS

Kenneth R. Avery

National Oceanographic Data Center

SILVER SPRING, MD.
February 1972

UDC 551.510.522:551.571.4:551.501.721:551.526.6

551.5	Meteorology
.501.721	Methods of observation and compilation of radiation
.510.522	Structure of boundary layer of troposphere
.526.6	Sea surface temperature
.571.4	Vertical distribution of humidity near earth's surface

CONTENTS

LITERATURE SEARCH FOR ATMOSPHERIC HUMIDITY PROFILE MODELS FROM THE SEA SURFACE TO 1,000 METERS

Kenneth R. Avery

ABSTRACT. A search of the literature published before 1970 was made to find temperature-humidity profiles from the sea surface to the 1,000 meter level in order to derive atmospheric corrections for low-level airborne infrared (8μ to 13μ) sea surface temperature measurements. There are no substantiated, globally applicable, models for the first 1,000 meters from the results of previous measurements. (The primary emphasis of most research studies has been on the 10-meter microscale boundary layers.) This investigation shows that future work should be directed toward deducing suitable low level atmospheric profile equations by a study of available ship weather data together with a detailed analysis of ocean weather ship radiosonde soundings (sea surface up to 1,000 meters), or by airborne experiments designed to derive a method for computing environmental corrections for radiometric measurement of sea surface temperature using flight-level measurements of air temperature and humidity.

INTRODUCTION

A search of the literature* published prior to 1970 was conducted to obtain low-level atmospheric temperature-humidity profile equations from the sea surface to 1,000 meters. The profiles are needed for determining an improved Airborne Radiation Thermometer (ART) atmospheric correction term. The search included investigations conducted during the period from 1930 through 1969. Various methods have been used by investigators to determine low-level temperature-humidity profiles. The majority of the measurements were made to heights of approximately 40 meters, and only a few analyses have been reported in the 1,000 meter altitude range of interest for ART corrections.

The earliest studies, in the 1930's, were made aboard ships at heights from just above the sea surface to forty meters. During World War II (1944-45), specially instrumented aircraft were used together with ships to gather meteorological data at altitudes above forty meters. In the 1950's and 1960's more sophisticated instrumented aircraft and other airborne platforms were used to acquire atmospheric measurements. Also, during this period some investigators resumed micrometeorological measurements to obtain data at the sea surface and in the adjoining air boundary layer just

---

*The literature search was undertaken while the author was assigned to the Airborne Remote Sensing Oceanography Project, U.S. Naval Oceanographic Office Research and Development Department.

a few meters above the water in order to study heat and momentum flux transfer between the sea and atmosphere.

GENERAL AREAS OF PROFILE INVESTIGATIONS

Investigations of the Atmosphere from the Sea Surface to 40 Meters

In the lowest zone above the water (0 to 40 meters) various scientists made measurements of temperature, humidity, vapor pressure, and wind speeds over the sea surface using similar techniques. These efforts were directed toward specific objectives such as computing the rate of evaporation (evaporation coefficient) (Montgomery 1940); the humidity gradient over the sea surface (Sverdrup 1946); vertical distribution of wind speed, temperature, and humidity above a water surface (Fleagle et al 1958); and the refractive index for radar wave propagation (Stephenson 1945). Additional efforts have been made by other investigators to develop theories for different air-sea interactions in the lower atmosphere; i.e., evaporation from the oceans, momentum transfer at the sea surface, and vertical diffusion in the lowest layers of the atmosphere.

Montgomery (1940) and Sverdrup (1946) agreed that vapor pressure is a linear function of the logarithm of height for stable and unstable atmospheric conditions up to 40 meters above the sea surface. In 1940, Montgomery introduced an equation representing the vertical gradient of vapor pressure as the nondimensional quantity Γ, which he called the evaporation coefficient and it assumes a logarithmic distribution:

$$\Gamma \equiv - \frac{1}{e_s - e_b} \frac{de}{d\ln z} \qquad (1)$$

where e_s = surface vapor pressure; e_b = any standard level for vapor pressure; Γ = vertical gradient of vapor pressure; z = height; e = vapor pressure.

One hundred and fifteen 10-minute-interval measurements were made from the ATLANTIS during its cruises off the eastern United States coast during the summer of 1935, and used as a data base by Montgomery to develop equation (1).

In 1946 Sverdrup (1946) elaborated on Montgomery's work. Using the evaporation coefficient (Γ) term, he developed an equation for computing the average vertical humidity gradient as a function of height z (to 30 meters) for stable and unstable atmospheric conditions. Temperature, vapor pressure, and wind observations were taken at the sea surface and three higher elevations (6.2m, 11.4m, and 27.6m) aboard the USS INDIANAPOLIS in 1937 by Lieutenant F. L. Black at Sverdrup's suggestion. Forty-six sets of these measurements were compiled for stable and unstable atmospheric conditions along a route from 33°36'N, 119°33'W (off the coast of California near San Diego) to areas northwest, east, and northeast of Hawaii to 57°19'N, 141°33'W (end point in Gulf of Alaska).

For unstable conditions the average vertical humidity gradient at any height z can be computed from Sverdrup's equation:

$$\frac{dq}{dz} = -\frac{\Gamma_a}{z}(q_s - q_a) \qquad (2)$$

where: q = humidity; z = height; Γ_a = evaporation coefficient at height a; q_a = humidity at height a; q_s = humidity at the sea surface; and Γ_a is from either equation (3) or equation (4).

With the assumption that the vertical transfer of water vapor is independent of height within the boundary layer, Montgomery (1940) obtains for a smooth surface:

$$\Gamma_a = \left(\frac{\lambda \nu k_o}{\kappa} + \ln \frac{k_o \gamma_o W_a a}{\kappa}\right)^{-1}, \qquad (3)$$

where λ is a numerical factor which occurs in the equation for the thickness, δ, of the laminar boundary layer and κ is the kinematic coefficient of diffusion of water vapor through air, ν is the kinematic viscosity of the air, k_o is von Karman's constant = 0.4, γ_o is a resistance coefficient, W_a is the wind velocity at height a, and a is the desired height above the sea surface. According to von Karman $\lambda = 11.5$, whereas Montgomery obtains $\lambda = 7.8$. With $\lambda = 11.5$ and a = 600 cm, the following numerical values of Γ apply at a temperature of 20°C:

ν	κ		Γ-values	
$cm^2 sec^{-1}$	$cm^2 sec^{-1}$	$W_6 = 2$	$W_6 = 4$	$W_6 = 6$ m sec^{-1}
0.15	0.15	0.087	0.0825	0.080

At 0°C the corresponding values are about one percent larger.

For a rough surface, independent of the wind velocity:

$$\Gamma_a = \left(\ln \frac{a+z_o}{z_o}\right)^{-1}, \qquad (4)$$

where a is the desired height above the sea surface, z_o is the roughness length.

A rough value of the humidity gradient under stable conditions can be found by using equation (2) and introducing a suitable Γ value from Figure 2.

Another micrometeorological observation program was conducted by Fleagle, Deardorff, and Badgley (1958) to obtain vertical profiles of wind speed, temperature, and vapor pressure. The observations were made in the center of East Sound during a four-day period in July 1958. East Sound is a salt water inlet approximately one mile wide, seven miles long, and 90 feet deep, and is located in the San Juan Archipelago between Vancouver Island and the mainland at about 40°North latitude. It is surrounded on three sides by Orcas Island opening to the south.

The wind speeds were measured at eight levels from 31 to 442 cm above the water and the dry and wet bulb temperatures were taken at four levels (40, 80, 160, and 320 cm). Average values of wind speed, temperature, and vapor pressure were determined for thirty 1-hour periods. The investigators characterized the vapor density profile by a profile number α expressed as:

$$\alpha_q = z \frac{\partial q}{\partial z} \Big/ (q - q_o), \qquad (5)$$

where q is the property of a single profile and q_o its surface value. Similar expressions hold for wind speed and temperature. From these measurements figure 3 gives α values for water vapor (α_e), temperature (α_t) and wind speed (α_u). The profile contour numbers for water vapor and temperature are represented in figure 3 by solid and open circles while the wind speed is shown as an X.

Fleagle states that the curvature of the vapor pressure profile is relatively independent of stability as indicated by the Richardson number (R_i) at the 80 cm level.

Paulson (1967) used data from observations made by University of Washington personnel as part of the International Indian Ocean Expedition during the period of February 26 to March 9, 1964, to obtain profiles of wind speed, temperature, and humidity. One hundred eighteen sets of simultaneous measurements were made at heights of 1 to 8 meters above the sea surface by instrumentation mounted on a specially designed buoy. Paulson showed that the humidity profile measured to eight meters over the Indian Ocean could be represented for the stable condition by:

$$q - q_o = \frac{q_*}{\alpha_e} \left[\ln \frac{z}{z_o} + \frac{\gamma}{4} \frac{z}{L'}\right] \qquad (6)$$

where $\frac{\gamma}{4} = 7.5 \pm 1.5$; $\frac{z}{L'} = \frac{R_i}{1 - \frac{\gamma}{4} R_i}$ and γ = an arbitrary

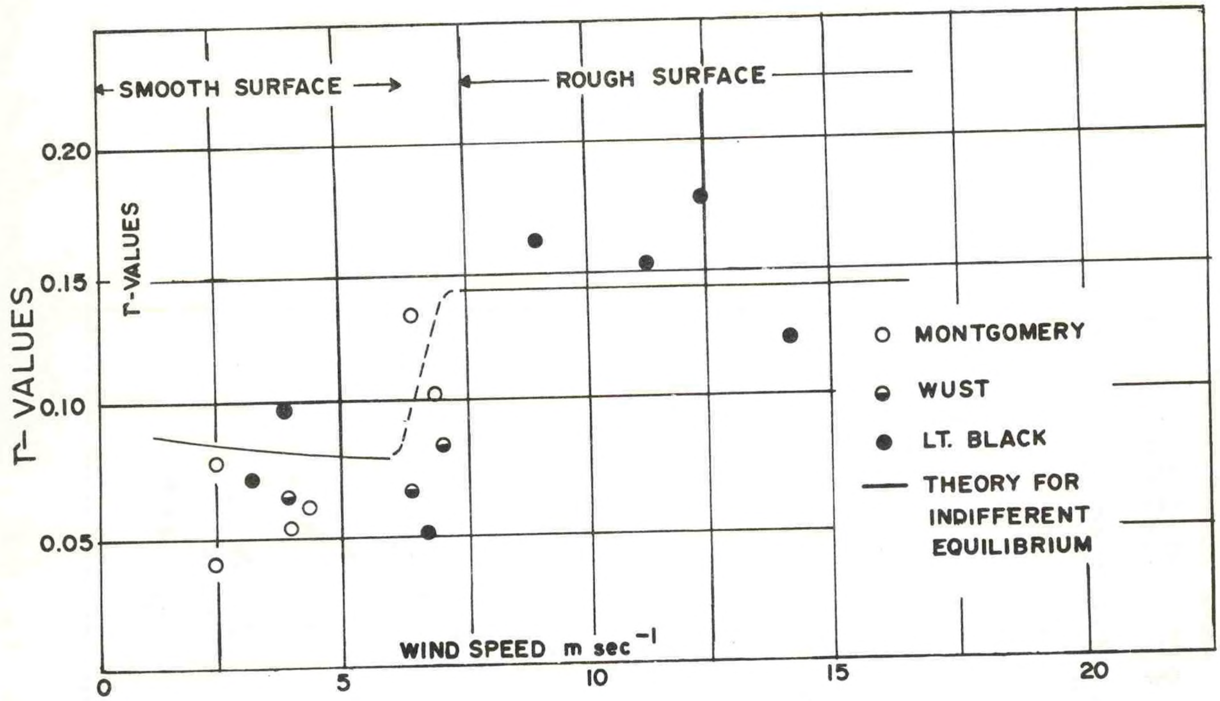

Figure 1.--Γ-values for instability.

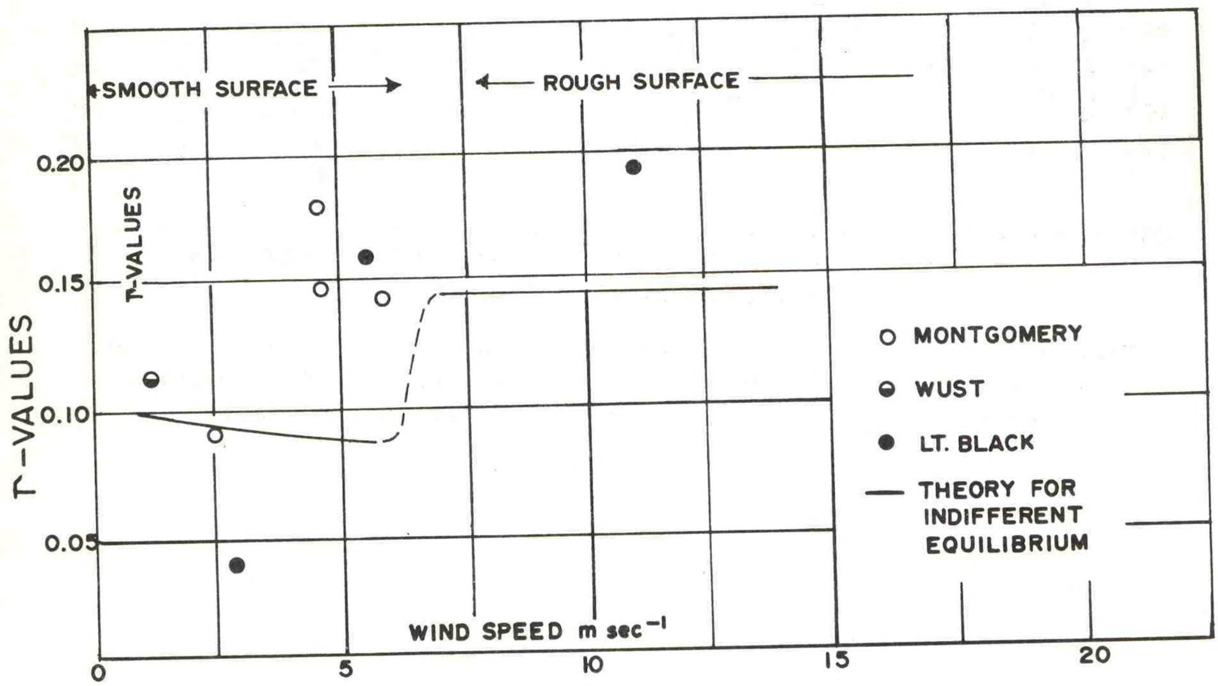

Figure 2.--Γ-values for stability.

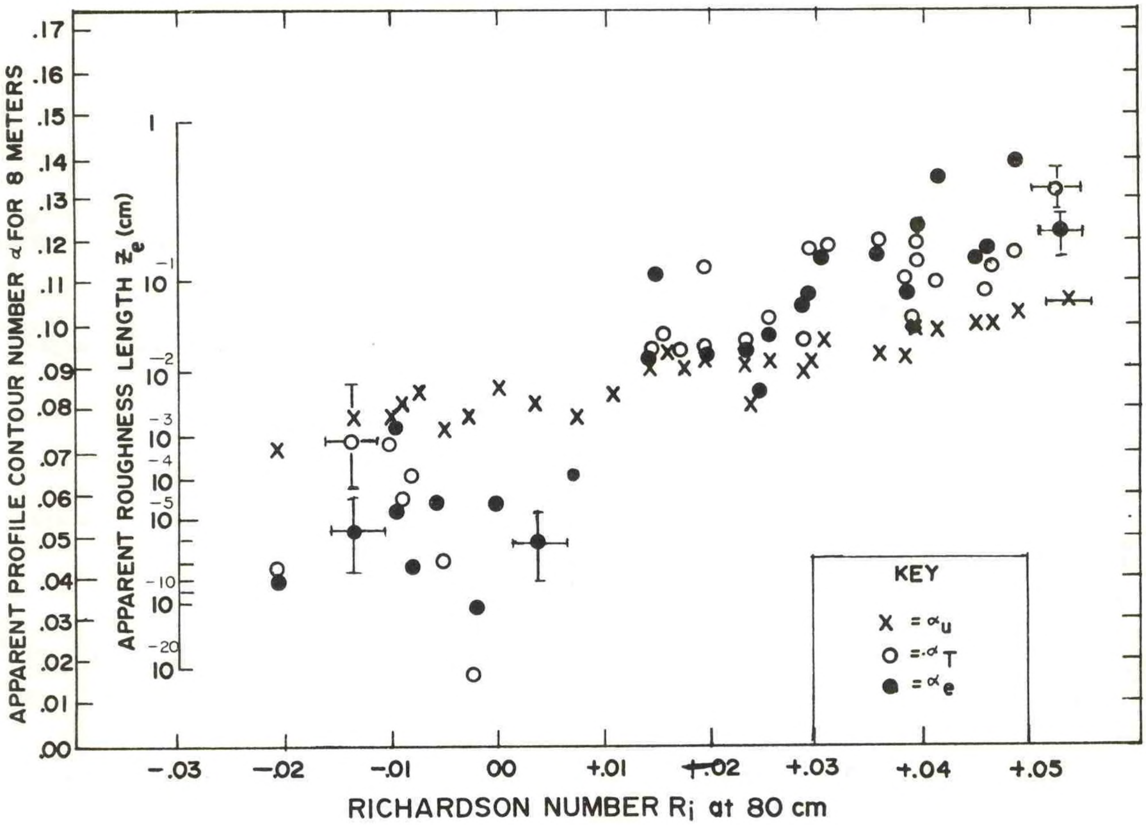

Figure 3.--A plot of profile contour number, α (a measure of the relative profile gradient) vs Richardson number, R_i, computed for 80 cm for wind, temperature, and water vapor density.

constant determined from the observations; q_* = specific humidity gradient; $\alpha_e = 1$; and $L' = \alpha_h L$ where α_h is assumed constant.

For the unstable case the humidity profile is depicted by Paulson from the Businger-Dyer representation as:

$$q - q_o = q_* \left[\ln \frac{z}{z_o} - \psi_1\right], \tag{7}$$

where $\psi_1 = 2 \ln \frac{1+\chi}{2} + \ln \frac{1+\chi^2}{2} - 2 \tan^{-1}\chi + \frac{\pi}{2}$, (8)

and $\chi = (1 - \gamma \frac{z}{L})^{\frac{1}{4}}$, (9)

where L is the Monin-Obukhov stability length (nondimensional parameter),

and $\frac{z}{L} = R_i$ and applies over a limited stability range.

Investigations of the Atmosphere Above 40 Meters Over the Sea Surface

The first use of an aircraft to make meteorological soundings of the atmosphere above 40 meters over the sea was made during July to October 1944 (Craig 1946). These observations were taken to gather information concerning the vertical distributions of temperature, humidity, and the refractive index near the sea surface for comparison with observed characteristics of radio transmissions. Nearly 500 soundings were made in air that had traveled less than 50 miles (since leaving land) over Massachusetts Bay in the lowest 1,000 feet above the water surface. From the 500 soundings, 51 were selected for discussion in this paper. They were studied individually in relation to weather data from nearby land stations to determine what meteorological processes had led to the observed vertical distributions. The author did not develop any equations for temperature and humidity profiles. Examples of Craig's data are shown in figure 4. The open circles depict the measurements made during the first aircraft ascent or descent and the smaller solid dots are the check measurements. The broken lines show the distributions the parameters would have in homogeneous air as compared with the observed distributions. The temperatures and dew point values at the sea surface and the surface potential index are shown by arrows. The air trajectory at 1,000 feet is shown by an arrow beginning at the coast line and terminates at the sounding point. On the characteristic diagram, the saturation curves for salt water (left curve) and fresh water (right curve) are located in the lower right hand corner. All the points including those for the check sounding are plotted and indicated by small dots. Each sounding has a characteristic curve and it terminates at the point on the saturation curve for salt water agreeing with the best estimate of the water temperature.

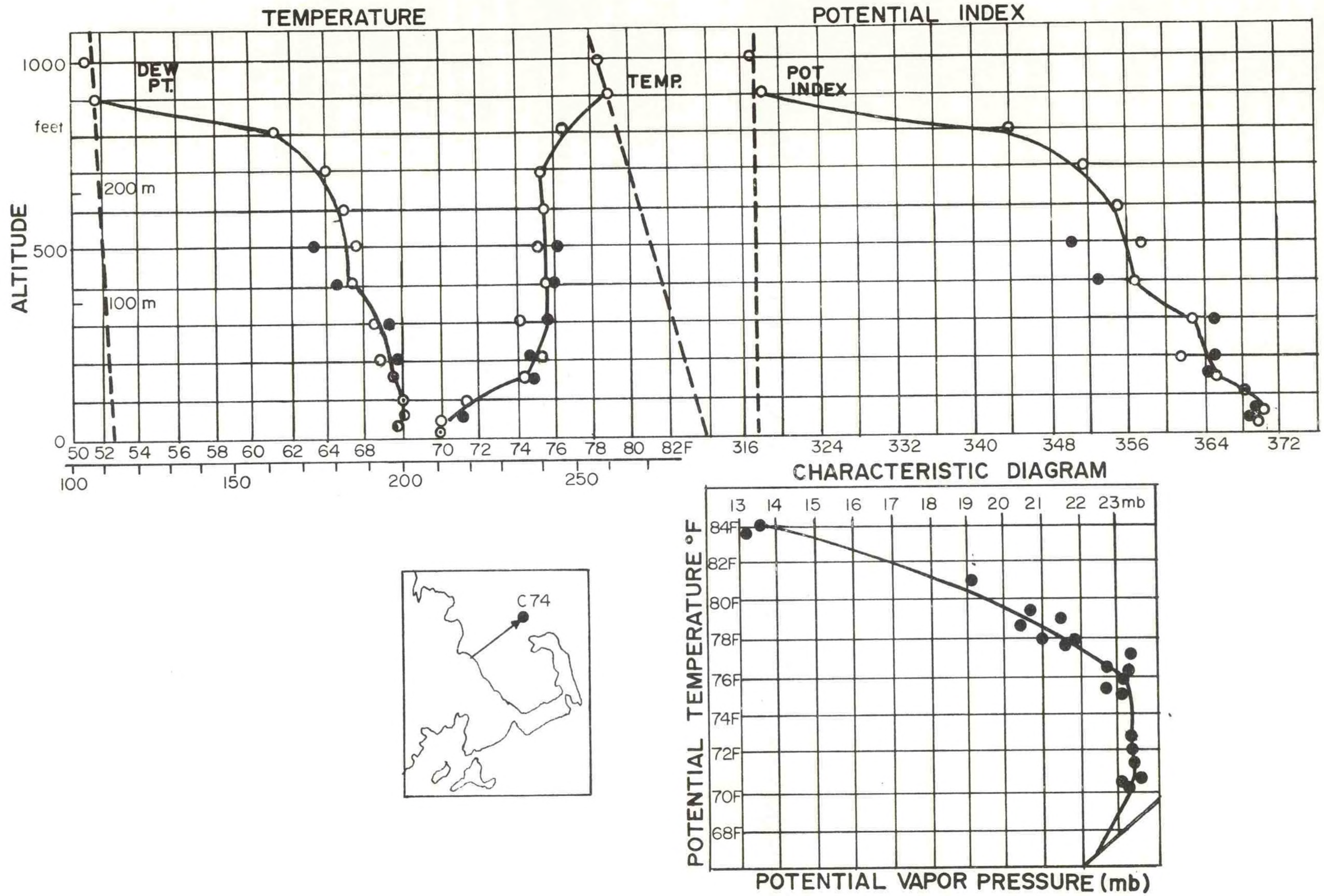

Figure 4.--C 74; 42°08'N, 70°16'W; 24 July 1944; o ascent 10^h45^m -10^h55^m, • ascent 10^h57^m-11^h02^m; wind-240°/16 mph at 1,000 ft., 2B (direction not observed) at surface (SSW at North Truro and South Weymouth); 1,000-ft. trajectory 24 mi., 1 1/2 hr., from Plymouth.

Between 1947 and 1949 additional papers were published by Craig (1947, 1949a, 1949b) using selected data acquired from the 1944 aircraft soundings mentioned above. These papers were concerned with the following: vertical temperatures and humidity distributions in the convective layer above the sea surface; the vertical eddy transfer of heat and water vapor in stable air; and the evaporation from the ocean into hydrostatically stable air.

Another aircraft sounding program (Emmons 1947) was undertaken in 1945 to collect meteorological data over the ocean between Nantucket and New Jersey covering a distance of 50 to 200 miles off shore. Ships were used to determine sea surface temperatures and weather observations at selected points to supplement the aircraft soundings. Thirty-two soundings were made by flying a PBY-6 Navy amphibian from about 50 feet above the sea surface to 1,500 feet. The primary purpose of obtaining the soundings was to investigate the meteorological conditions influencing the propagation of ultrashort radio waves. The report gives a graphical and explanatory presentation of the results of the observations.

Each sounding was plotted to show the temperature and dewpoint temperature curves plus the corresponding potential index curve. The values of the potential refractive index were computed from the formula used by Craig (1946). A Taylor diagram (Montgomery 1951) of potential temperature and potential vapor pressure is depicted for each sounding. The curve on the Taylor diagram can be used to define the water temperature for sea water of salinity 35 per mille. In the majority of the soundings the temperature and humidity measurements in the modified layer form a series of points that generally fit a straight line on the Taylor diagram.

Figure 5 is an example of Emmons' (1947) work. The aircraft's first ascent is indicated by circles and the second ascent is shown by dots. The dashed lines indicate temperature, dew point, and potential index lapse rates in homogeneous air and these are included for purposes of comparison with the observed lapse rate. Arrows on the diagram base point out the inferred sea surface values. On the Taylor diagram a number indicating the height in feet of the over-water modification is entered next to the appropriate point on the characteristic curve.

In the spring of 1946 an aircraft sounding project was conducted in the atmosphere's lowest 10,000 feet over the Caribbean Sea (Bunker et al 1949). Most of the dry- and wet- bulb temperature measurements were taken at 19°30'N, 66°W (50 miles north of San Juan, Puerto Rico), while others were taken at 10°N, 79°30'W (north of Coco Solo, Panama). Ships were used to measure sea surface temperatures plus surface air temperatures (dry- and wet-bulb) usually within a 20-mile radius of the aircraft soundings. The vertical soundings were flown in clear and cloudy areas above the sea. In addition, horizontal traverses were made for a duration of 5 to 30 minutes at approximately 100 knots airspeed in the vicinity of the vertical soundings.

This paper described the vertical distribution of temperature and humidity. Figure 6 is characteristic of the soundings considered during this project (Bunker et al 1949).

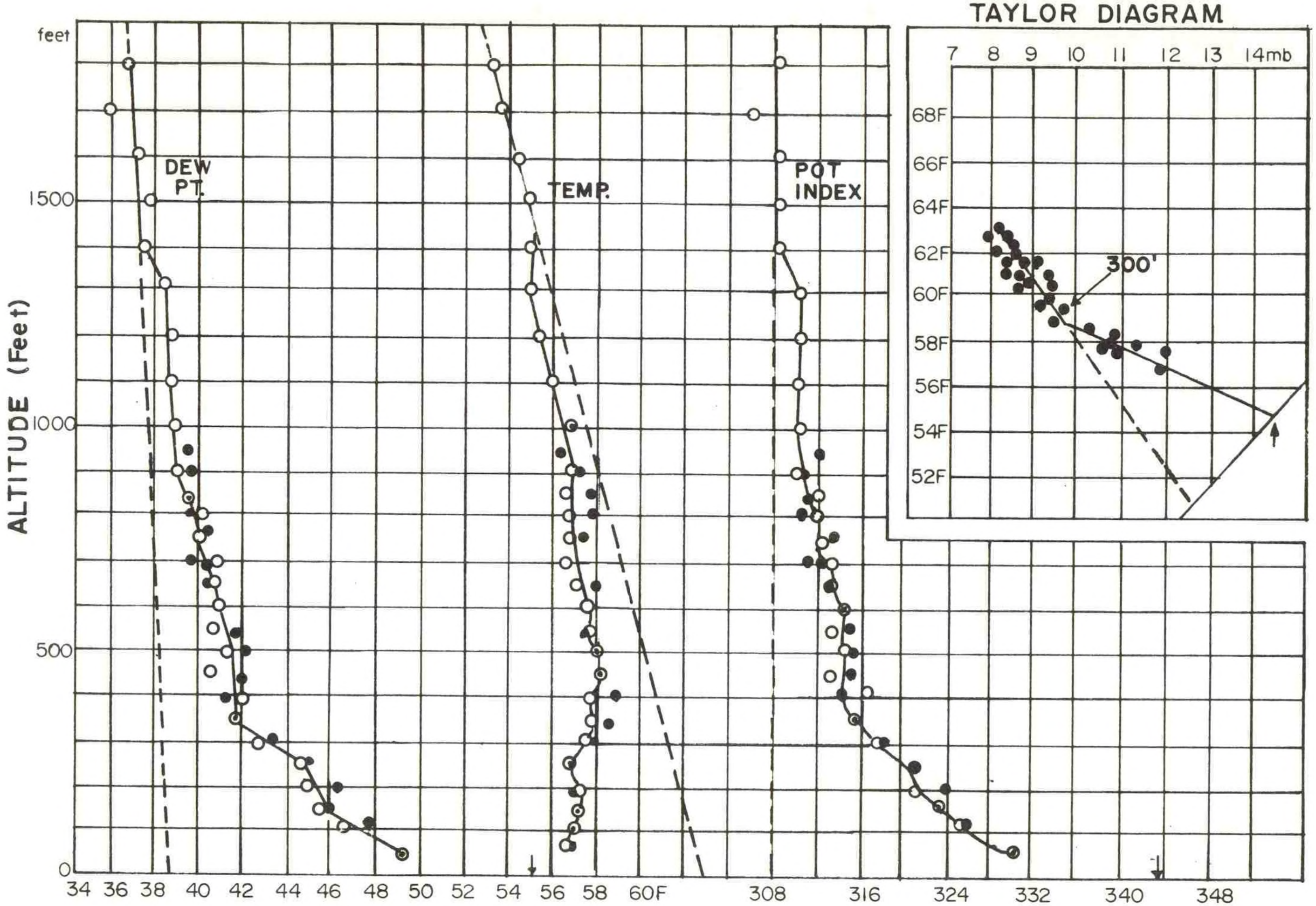

Figure 5.--Sounding 5; 40°18'N, 73°02'W; 6 June 1945; o ascent 16^h44^m–17^h05^m, ● ascent 17^h08^m–17^h21^m. The air has been cooled and moistened only to a height of 250 ft. by passage over the ocean. The stable region between 250 ft. and 900 ft. is the result of sheering stratification.

The humidity distribution can be computed by numerical integration from the following equation:

$$\delta q/\delta z = C \exp (W_o h/K''' \pi)\cos(\pi z/h), \qquad (10)$$

where C is a constant (flux of water vapor); W_o is a positive constant (vertical velocity); K''' is an assumed constant in the layer (coefficient of eddy diffusivity); z is a selected height; h is the cloud layer height; and q is the humidity.

The theoretical curve of figure 6, calculated with W_o/K''' being 0.052 x $10^{-3} cm^{-1}$, shows the essential features of the humidity distribution; that is, the rapid decrease upward through the stable layer and the slowly decreasing humidity in the cloud layer.

Other Investigations To Develop Atmospheric Profiles

During the period of 1950 to 1969 many new attempts have been made by scientists toward solving problems related to various atmospheric profiles. The following investigations illustrate a few of the approaches made by different investigators over the past 20 years.

Hutcherson's (1965) study attempts to acquire an estimate of the atmospheric moisture content in a form compatible with the needs of analyses concerned with the evaluation of infrared detection devices operating within the atmosphere. He presents profiles of absolute humidity for standard and nonstandard days together with tabulations of precipitable water for these conditions. The results are valid for only middle latitudes and altitudes from sea level to 100,000 feet.

Precipitable water (W) may be calculated from absolute humidity (A) or water vapor density and this is the basis for the calculations in his study. The following expression for precipitable water (W) assumes that absolute humidity is a function of its position along the radiation path:

$$W = 0.3048\int_{r_o}^{r} A\,dr, \qquad (11)$$

where A = absolute humidity in g/m^3; r_o = one end of the radiation path; r = any arbitrary position along the radiation path (the distance between r and r_o is measured in feet); W = precipitable water between r_o and r measured in microns ($1\ \mu = 10^{-6}m$).

Whenever the absolute humidity (A) is independent of position, the integral becomes a simple product and

$$W = 0.3048A(r - r_o), \qquad (12)$$

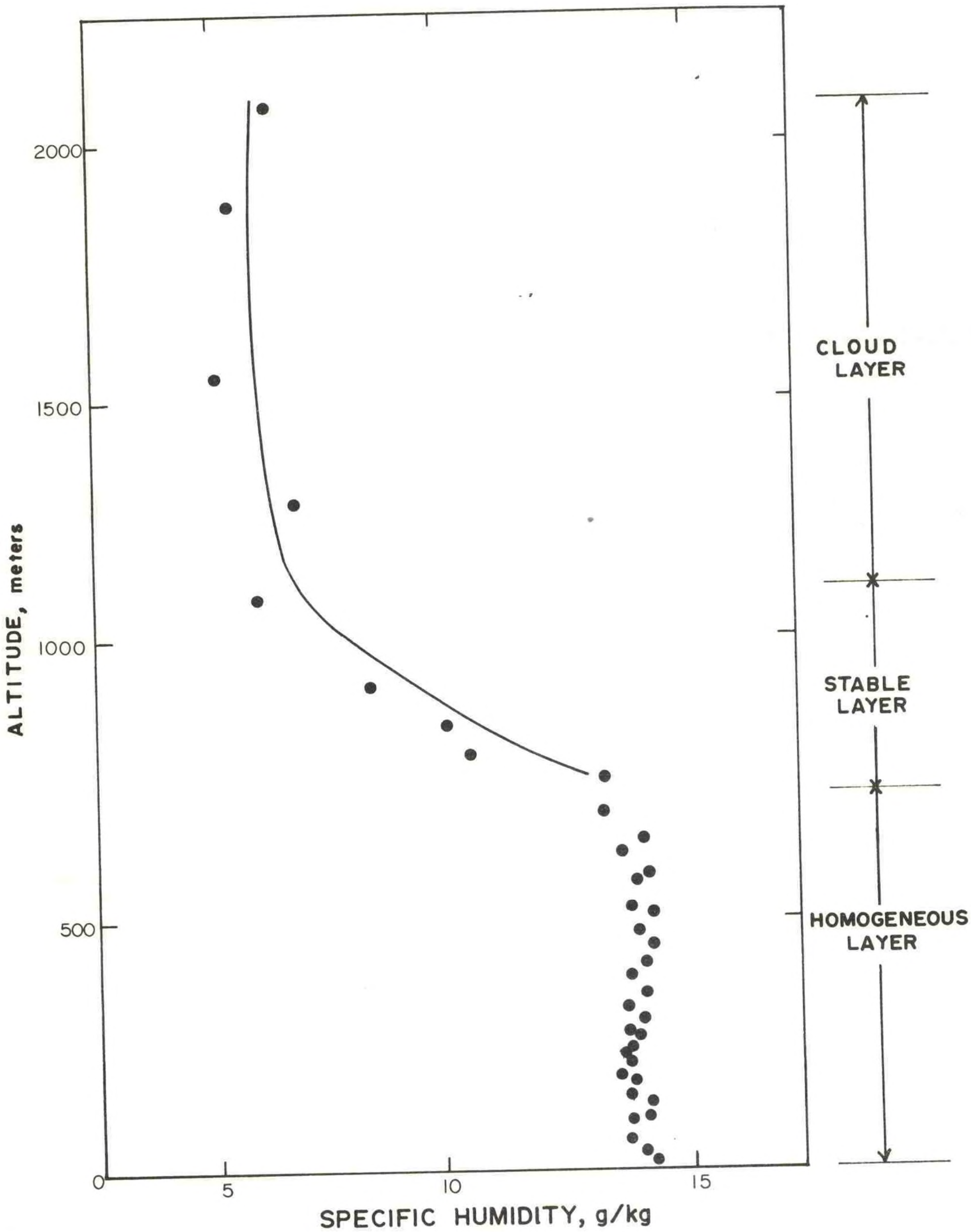

Figure 6.--Humidity distribution in the cloud layer on 27 April 1946, 1025 AST.

If a vertical path that extends from an altitude h_o upward to another altitude h is known, then the absolute humidity becomes a function of altitude. Consequently, precipitable water can be related to absolute humidity by the equation:

$$W_z = 0.3048\int_{h_o}^{h} A\,dh, \tag{13}$$

where the path length is the altitude difference between h_o and h in feet.

When there is another path with an angle (Θ) from the vertical between altitudes h_o and h, then:

$$W_\Theta = \frac{W_z}{\cos\Theta}, \tag{14}$$

where W_Θ is the precipitable water in the inclined path and Θ is less than 90 degrees. For this equation a flat earth is assumed and it introduces a negligible error. If precipitable water amounts were known, then charts and tables are available in the Smithsonian Meteorological Tables (1951) that list transmission coefficients as functions of precipitable water and wave length. But, these tabulations can be considered valid for only standard conditions of pressure and temperature. Therefore, a correction is required before precipitable water can be used to read the tabulations whenever the pressure varies from the standard. The term "reduced absolute humidity" denoted by $A\sqrt{P/P_o}$ can be used to correct precipitable water for pressure variations. Inserting $A\sqrt{P/P_o}$ into equations (11) through (14) results in the following expressions for precipitable water (W') corrected for pressure:

$$W' = 0.3048\int_{r_o}^{r} A\sqrt{P/P_o}\,dr \tag{15}$$

$$W' = 0.3048A\sqrt{P/P_o}\,(r-r_o) \tag{16}$$

$$W'_z = 0.3048\int_{h_o}^{h} A\sqrt{P/P_o}\,dh \tag{17}$$

$$W'_\Theta = \frac{W'_z}{\cos\Theta} \tag{18}$$

Using the above to obtain W', it is possible to go straight to the tabulations of standard condition coefficients.

TABLE 1. PRECIPITABLE WATER--STANDARD DAY

h (ft x 10^{-3})	ΔW (μ)	W (μ)	ΔW' (μ)	W' (μ)
2	3538	3538	3488	3488
4	2662	6200	2533	6021
6	2011	8211	1804	7825
8	1496	9707	1310	9135
10	1119	10825	996	10131
12	814	11639	723	10854
14	582	12221	466	11320
16	415	12635	307	11627
18	277	12912	200	11827
20	178	13090	133	11960
22	122	13212	82.3	12042
24	79.1	13291	51.8	12094
26	51.6	13342	32.4	12126
28	31.6	13374	19.2	12145
30	17.6	13392	10.9	12156
32	10.2	13402	5.96	12162
34	6.50	13408	3.34	12166
36	4.40	13413	2.04	12168
38	2.95	13416	1.31	12169
40	2.12	13418	.880	12170
42	1.54	13419	.664	12171
44	1.28	13421	.516	12171
46	1.02	13422	.397	12172
48	.873	13422	.310	12172
50	.719	13423	.254	12172
52	.655	13424	.213	12172
54	.582	13424	.183	12173
56	.532	13425	.162	12173
58	.510	13425	.146	12173
60	.510	13426	.141	12173
62	.536	13426	.138	12173
64	.560	13427	.137	12173
66	.588	13428	.137	12173
68	.618	13428	.137	12174
70	.649	13429	.137	12174
72	.680	13430	.137	12174
74	.707	13430	.137	12174
76	.746	13431	.137	12174
78	.778	13432	.137	12174
80	.817	13433	.137	12174
82	.853	13433	.137	12174
84	.890	13434	.137	12175
86	.939	13435	.137	12175
88	.985	13436	.137	12175
90	1.04	13437	.137	12175
92	1.08	13438	.137	12175
94	1.13	13440	.137	12175
96	1.19	13441	.137	12175
98	1.24	13442	.137	12176
100	1.30	13443	.137	12176

Columns W and W' (precipitable water) are in microns (μ) where 1μ = 10^{-4}gm/cm^2.

TABLE 2.--PRECIPITABLE WATER-SYNTHETIC WET DAY

h (ft x 10^{-3})	ΔW (μ)	W (μ)	ΔW' (μ)	W' (μ)
2	6995	6995	6913	6913
4	5128	12123	5034	11947
6	3834	15956	3563	15510
8	2847	18803	2533	18043
10	2099	20902	1816	19859
12	1590	22492	1276	21135
14	1138	23630	880	22015
16	861	24491	635	22649
18	631	25122	444	23094
20	442	25564	308	23402
22	312	25876	204	23605
24	211	26087	136	23741
26	138	26225	84.8	23826
28	81.7	26307	53.2	23879
30	50.0	26357	32.8	23912
32	29.0	26386	19.6	23932
34	18.0	26404	11.6	23943
36	11.5	26416	6.91	23950
38	7.67	26423	3.77	23954
40	5.86	26429	2.38	23956
42	4.27	26433	1.69	23958
44	3.24	26437	1.26	23959
46	2.55	26439	.980	23960
48	2.11	26441	.779	23961
50	1.80	26443	.641	23961
52	1.60	26445	.522	23962
54	1.39	26646	.438	23962
56	1.28	26447	.376	23963
58	1.23	26449	.343	23963
60	1.22	26450	.331	23964
62	1.25	26451	.324	23964
64	1.37	26452	.326	23964
66	1.45	26454	.326	23964
68	1.52	26455	.326	23965
70	1.59	26457	.326	23965
72	1.67	26469	.327	23965
74	1.75	26460	.328	23966
76	1.84	26462	.329	23966
78	1.93	26464	.329	23966
80	2.02	26466	.329	23967
82	2.12	26478	.330	23967
84	2.23	26470	.330	23967
86	2.34	26473	.332	23968
88	2.45	26475	.333	23968
90	2.58	26478	.333	23968
92	2.71	26481	.334	23969
94	2.85	26483	.335	23969
96	2.98	26486	.335	23969
98	3.12	26489	.335	23970
100	3.27	26493	.336	23970

TABLE 3.--PRECIPITABLE WATER-SYNTHETIC DRY DAY

h (ft x 10^{-3})	ΔW (μ)	W (μ)	ΔW' (μ)	W' (μ)
2	1815	1815	1747	1747
4	1345	3160	1266	3013
6	980	4140	893	3906
8	709	4848	622	4528
10	524	5373	483	5011
12	378	5750	338	5349
14	270	6020	234	5583
16	192	6212	159	5742
18	134	6347	105	5847
20	91.8	6438	68	5915
22	60.7	6499	41	5956
24	37.2	6536	25	5981
26	21.5	6558	14	5995
28	12.5	6582	7.0	6002
30	6.73	6589	3.3	6005
32	3.96	6593	1.9	6007
34	2.32	6595	1.3	6008
36	1.53	6597	.79	6009
38	1.08	6598	.52	6009
40	.811	6599	.36	6010
42	.628	6600	.26	6010
44	.500	6600	.20	6010
46	.402	6600	.15	6010
48	.341	6601	.13	6010
50	.295	6601	.11	6011
52	.259	6601	.095	6011
54	.234	6602	.078	6011
56	.219	6602	.070	6011
58	.216	6602	.061	6011
60	.216	6602	.057	6011
62	.221	6602	.055	6011
64	.230	6603	.055	6011
66	.240	6603	.055	6011
68	.250	6603	.056	6011
70	.261	6603	.056	6011
72	.272	6604	.056	6011
74	.285	6604	.056	6011
76	.298	6604	.055	6011
78	.311	6605	.055	6011
80	.325	6605	.055	6011
82	.340	6605	.054	6011
84	.355	6606	.054	6011
86	.371	6606	.054	6012
88	.386	6606	.054	6012
90	.402	6607	.054	6012
92	.419	6607	.053	6012
94	.438	6608	.053	6012
96	.456	6608	.053	6012
98	.475	6609	.053	6012
100	.495	6609	.053	6012

Columns W and W' (precipitable water) are in microns (μ) where 1 μ = 10^{-4}gm/cm2.

A synthetic wet day is defined as one that will have more moisture than 90 percent of all days at a specific altitude. Whereas, the synthetic dry day contains less moisture than 90 percent of all days at a specific altitude. Figure 7 presents the profiles of synthetic wet and dry days plus a mean annual absolute profile showing a standard day.

Figure 8 shows the synthetic and mean profiles of the "reduced absolute humidity" parameter necessary in the W' computations. The same definitions of the dry and wet day prevail. All the $\sqrt{P/P_0}$ values were acquired from the 1962 Revised United States Standard Atmosphere.

Hutcherson's (1965) results are given in tables 1, 2 and 3. The values of W_z and W_z' are for altitudes from sea level to 100,000 feet and the tabulations are valid for only middle latitudes due to data limitations. In the three tables the ΔW and ΔW' columns are precipitable water in microns contained in the 2,000-foot layer just below the altitude listed. Columns W or W' give the total amount of precipitable water in microns that exist from sea level to a particular altitude.

Table 1 gives values for the standard day and tables 2 and 3 represent values for the synthetic dry and wet day. The values for the three tables were obtained by graphically integrating the profiles in figures 7 and 8. The values in the W and W' columns were carried up to five digits but the accuracy is probably lacking past the third digit. Comparing these results with other precipitable water studies indicated no conspicuous differences.

Table 4 compares the atmospheric transmission at 7.4μ, 10.3μ, and 13.2μ as obtained from the Smithsonian Meteorological Tables (1951) No. 146 for precipitable water values corresponding to wet, standard, and dry days. The 8 to 13μ infrared window is commonly used for radiation sea surface temperature measurements. These estimates indicate a decrease of atmospheric transmission of 6.2 percent at 10.3μ between wet and dry days at midlatitudes. This transmission difference would be interpreted as a percentage error in the estimation of the absolute temperature of the emitting surface. While these transmission coefficients are not directly applicable to airborne measurements, they provide a first estimate of the effect of atmospheric water vapor upon sea surface radiation temperature measurements.

Table 4.--Atmospheric transmission*

WAVE LENGTH	PRECIPITABLE WATER, 0 to 2,000-FT LAYER			
	WET DAY 6.913mm	STANDARD DAY 3.488mm	DRY DAY 1.747mm	PRECIP. WATER VALUES FROM TABLES 1, 2, 3
7.4μ	(6mm) 10.9%	(3.1mm) 20.6%	(2.1mm) 27.2%	(TABLE 146 TABULAR VALUES)
10.3μ	(6.2mm) 92.5%	(3.3mm) 94.5%	(2.1mm) 98.7%	(TABLE 146 TABULAR VALUES)
13.2μ	(6.7mm) 72.8%	(4.1mm) 67.1%(?)	(1.3mm) 76.7%	(TABLE 146 TABULAR VALUES)

*From Smithsonian Meteorological Tables (1951), Table No. 146, pp. 433-436.

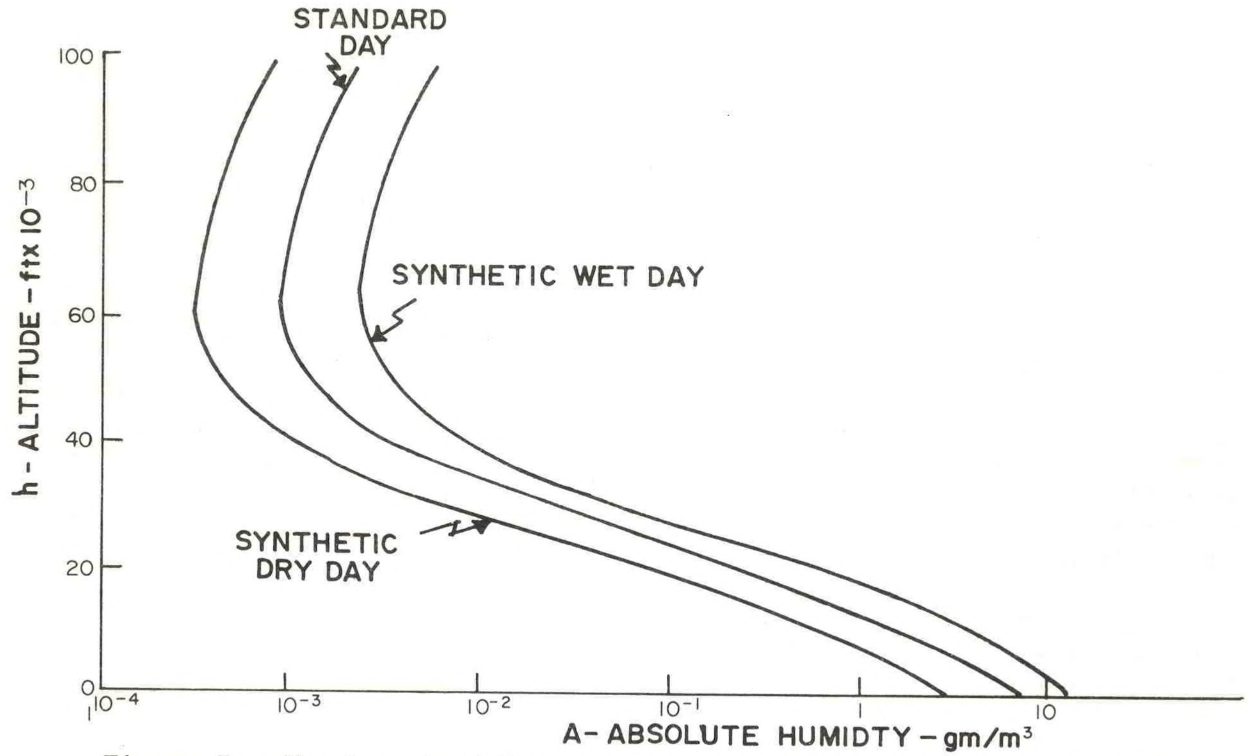

Figure 7.--Absolute humidity as a function of altitude for the middle latitudes and for standard, wet, and dry days.

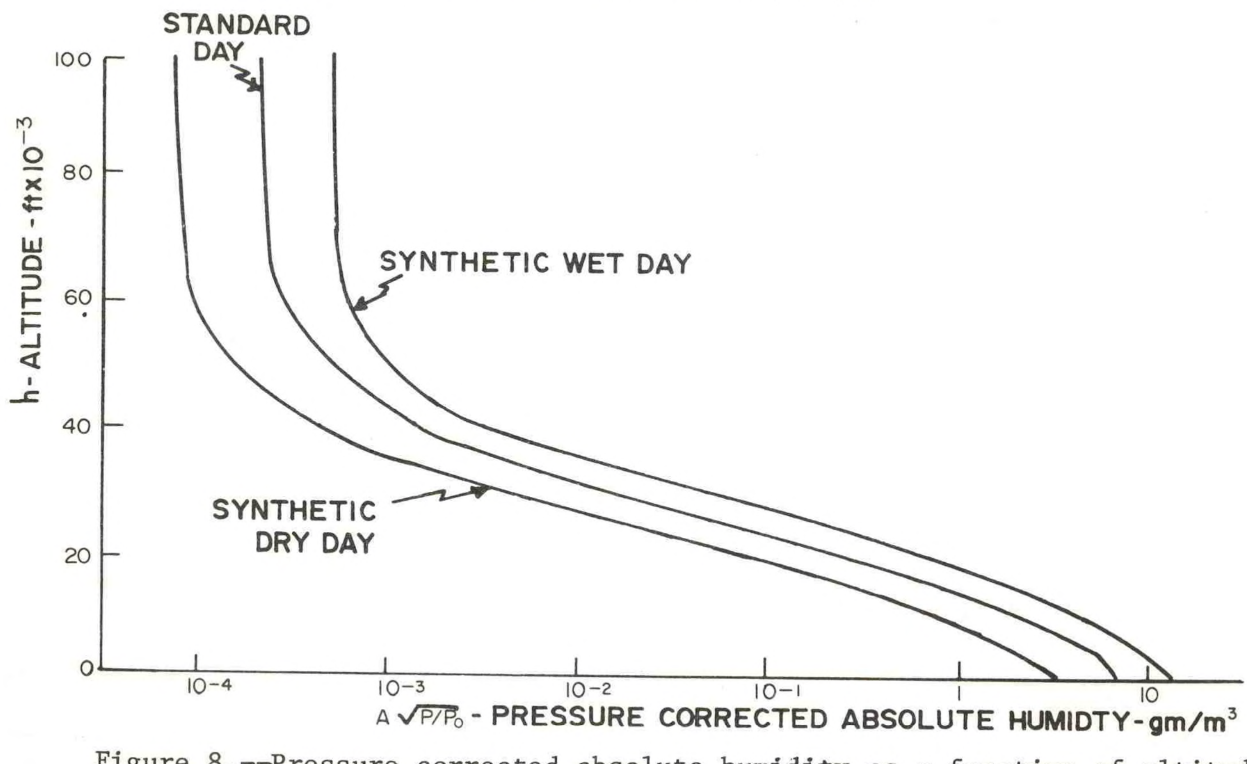

Figure 8.--Pressure corrected absolute humidity as a function of altitude for the middle latitudes and for standard, wet, and dry days.

On July 14, 1965 Kuhn (et al 1967) performed an aircraft radiometric sounding over Lake Superior, twenty miles east of Duluth, Minnesota. Two radiometers were used to make simultaneous measurements of 7.35 to 13.6μ (IRW) and 4.38 to 20.8μ (IRF upward irradiance) bands. Also, altitude and air temperature recordings were made together with visual surface observations.

The radiative power transfer equation may be subjected to an iterative solution to produce atmospheric water vapor distributions as a function of remote radiant power measurements over different infrared spectral ranges. The purpose of the Kuhn et al research is to study such a solution employing remote aircraft measurements of radiant power. The method reported requires observations of temperature, height, and spectral irradiance at a number of different altitudes (nine altitudes were flown during the July 14, 1965 flight). Two Barnes Engineering Company radiometers sensitive to different spectral intervals made up the sensor capability. One of the radiometers measured the spectral component of the upward infrared irradiance of flux-density at 4 to 20μ (IRF) while the other radiometer at 7 to 13μ (IRW) monitored the air-surface interface temperature. Both instruments measured the radiation in watts/m^2.

Irradiance and temperature data are inputs to a transfer solution for spectral irradiance moving upward in a plane parallel gaseous atmosphere. This equation can be shown as:

$$F = -\int_{\nu_1}^{\nu_2}\int_{z_1}^{z_2} B_\nu \left|\frac{\partial T_\nu(z)}{\partial z}\right| dz\, d\nu + \int_{\nu_1}^{\nu_2} B\nu_o \left[\int_{z_1}^{z_2} \left|\frac{\partial T_\nu(z)}{\partial z}\right| dz\right] d\nu \qquad (19)$$

where:

o = surface condition

F = irradiance (watts/meter^2 or microwatts/centimeter^2)

ν = wave number (reciprocal centimeters)

z = height (feet)

B = blackbody irradiance

T_ν = spectral transmissivity

W = mixing ratio for water vapor (grams/kilogram)

An iteration procedure requires the insertion of a progressive series of trial values of $T_\nu(z)$ in equation (19) until the calculated component of spectral irradiance is equal to the measured component of the upward irradiance. One must start with a trial value of W since $T_\nu(z)$ is equal to T(W). Finally, the iteration procedure will converge to the last value which is assumed to be the actual mixing ratio (W) at a particular observation level. The use of narrow and broad band (window) chopper bolometers results in surface temperatures that can be observed from an inflight aircraft. Only a vertical sounding is necessary to record these temperatures.

In solving equation (19) for water vapor, the upward irradiance component, F, is measured coming from a reception cone with a solid angle opening of $\Delta w = 2\pi \cos\Theta \sin\Theta \Delta\Theta$ where Θ is the nadir angle of a downward-looking radiometer. Also, $\Delta\Theta$ is defined as the radiometer's half beam width.

Figure 9 shows the curves for the filter transmissivities. Curve A is for the interface monitor covering the temperature radiometer (transmissivity of the infrared window) and curve B covers the transmissivity of the infrared irradiance (broad band) radiometer.

The equation for measured irradiance ($\overline{F}']_{\nu_1}^{\nu_2}$) can be expressed as:

$$\overline{F}']_{\nu_1}^{\nu_2} = \Delta W \int_{\nu_1}^{\nu_2} I_\nu \phi_\nu d\nu \qquad (20)$$

where ϕ_ν is the spectral sensitivity of the radiometer. Both the IRF and IRW radiometers were calibrated against a black-body source. The radiometers used in this experiment had solid opening angles (Δw) of 3 and 30 degrees for the IRW and IRF radiometers respectively. Figure 10 presents the results of the computer-model black-body calibrations of the two radiometers.

Figure 11 is a computer solution for the IRW altitude correction required when using the 7.4 to 13.2μ filter assuming mean monthly soundings. The IRW observed temperatures as a function of altitude over Lake Superior near Duluth are shown in figure 12. The data represents the same track but different altitudes up to 6,600 feet above the surface.

Figure 13 depicts the effects of a total optical mass of 0.1 to 1.0 gram/cm^2, at an average temperature 10°C through a 3,000 feet altitude layer. There is a significant change in the atmospheric transmission in the 7.3 to 9.4μ and 12.0 to 13.6μ ranges as the optical mass increases to 1.0 gram/cm^2.

Kuhn et al (1967) have used an iterative technique of determining the atmospheric humidity profile by the radiative transfer equation (19) to obtain irradiance as measured by the IRF and IRW radiometers. A mean climatological value for the water vapor mixing ratio is assumed as the initial value for an approximation of the spectral transmissivity [$T_\nu(z)$] in the radiative transfer equation. The water vapor profile [hence $T_\nu(z)$] is varied to bring the computed values of irradiance into agreement with the measured values from the IRW and IRF radiometers. The iteration is ended when the computed values reach a convergence limit of 100 μw/cm^2 of the measured values (which is the resolution limit of the instruments). The average computer (CDC 3600) solution time is 15 seconds for a ten-level solution over the spectral range of 4.39 to 20.83μ. The results shown in figure 14 for the determination of the water vapor profiles from the Lake Superior flights

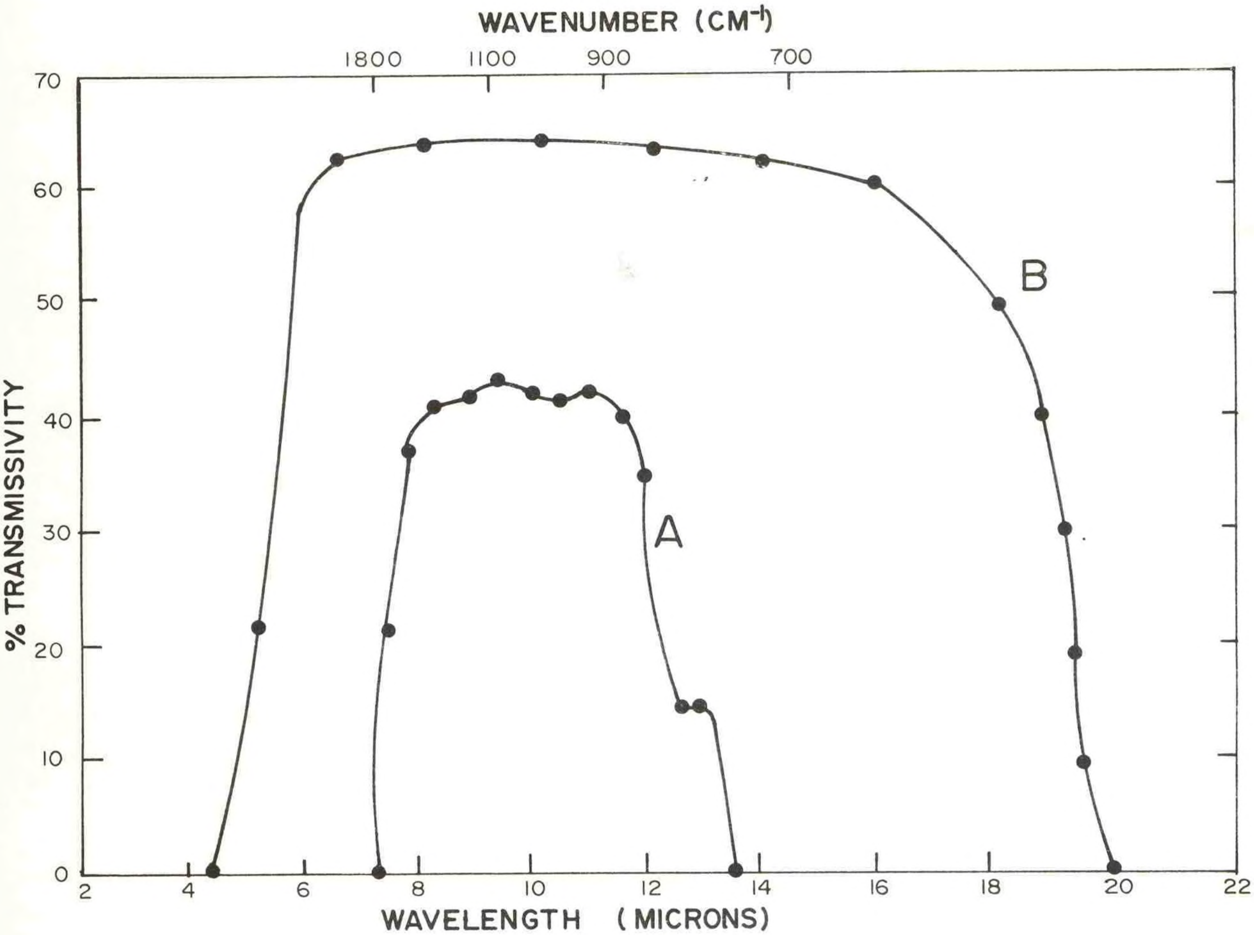

Figure 9.--Filter transmissivities for the interface monitor (A) and the broad band radiometer (B).

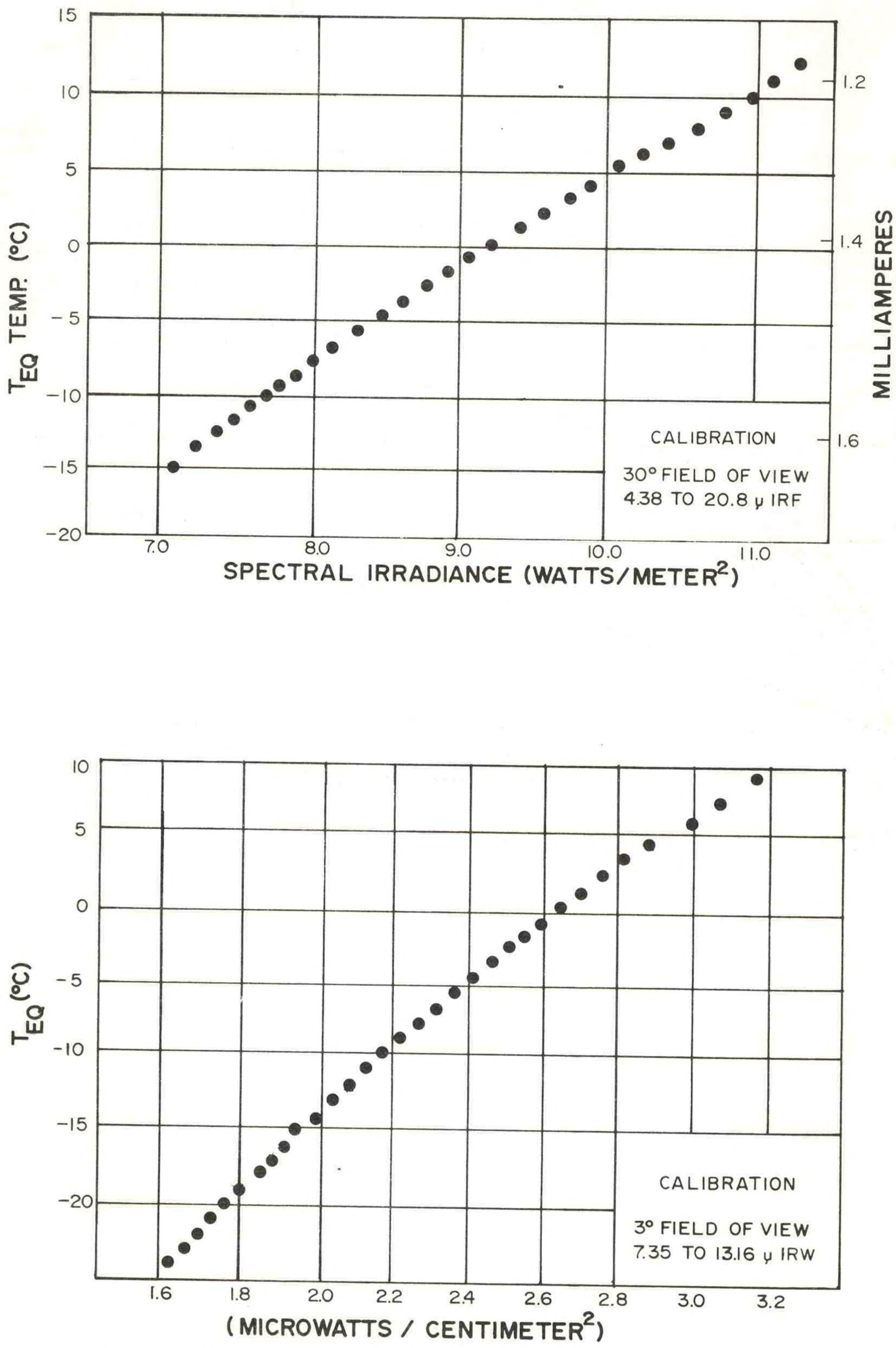

Figure 10.--Computer model calibrations, IRW and IRF.

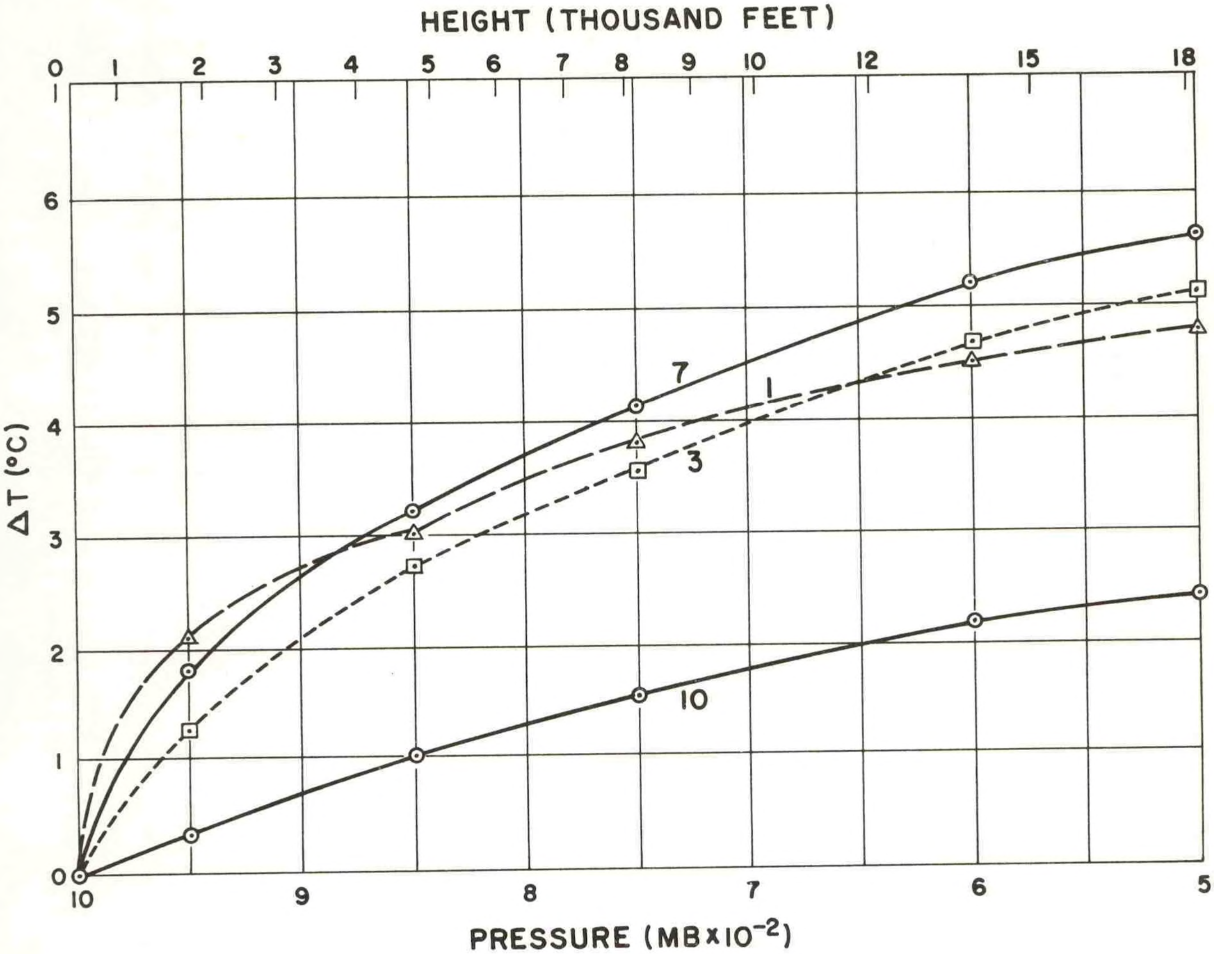

Figure 11.--Computed altitude corrections, IRW, Sault Ste. Marie (SSM).

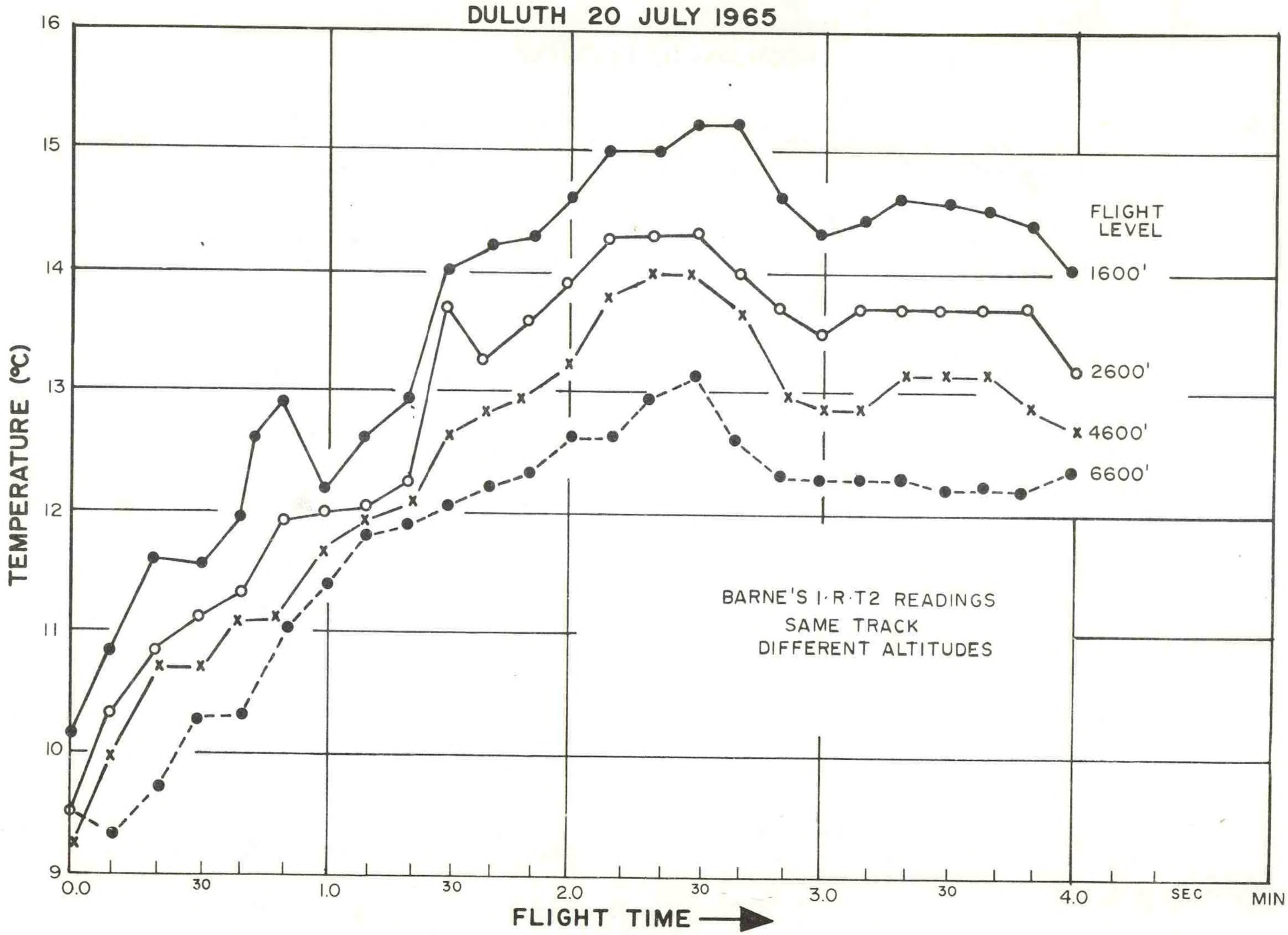

Figure 12.--Observed altitude corrections, IRW, Duluth (DLH).

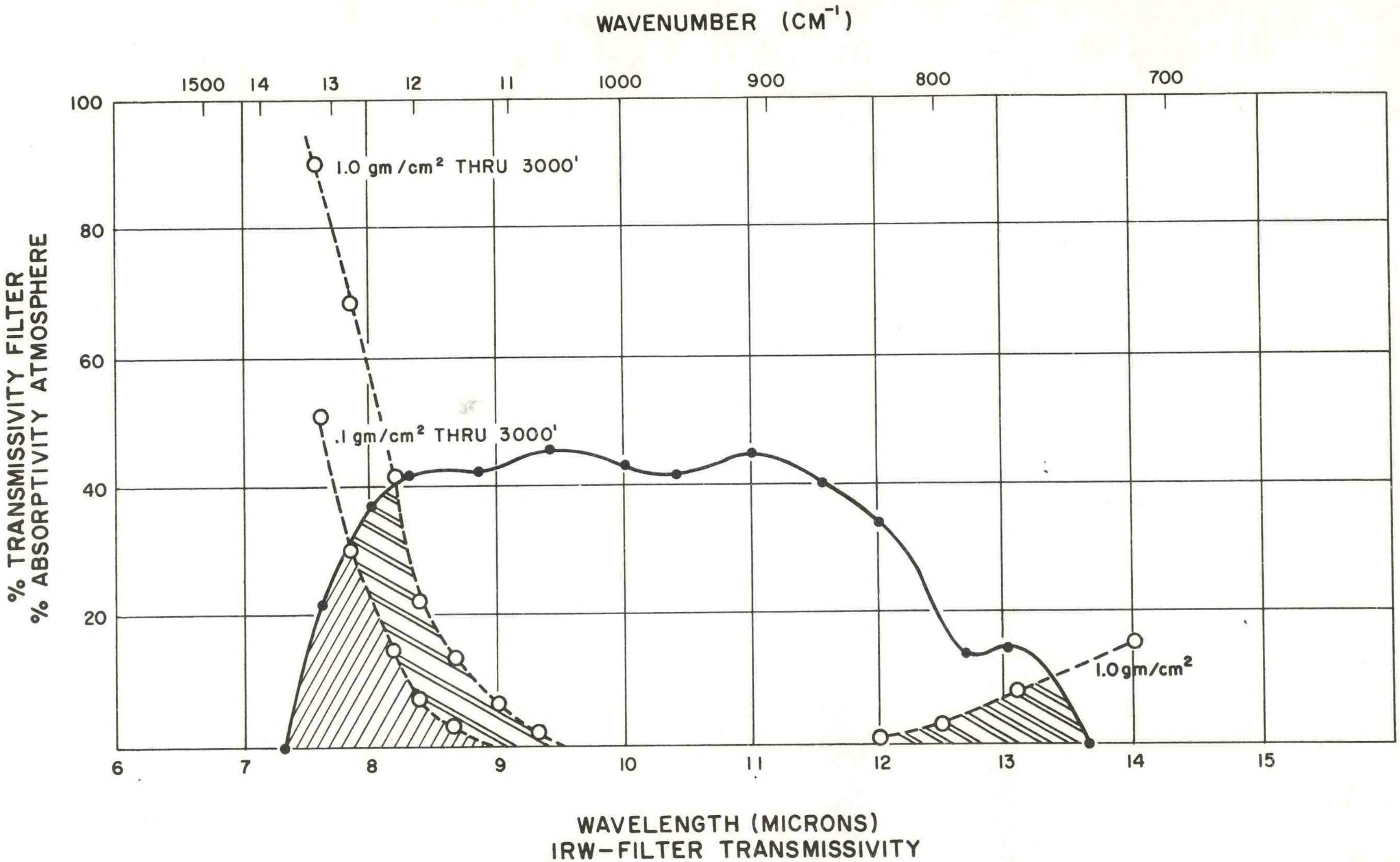

Figure 13.--Atmospheric effects on IRW filter.

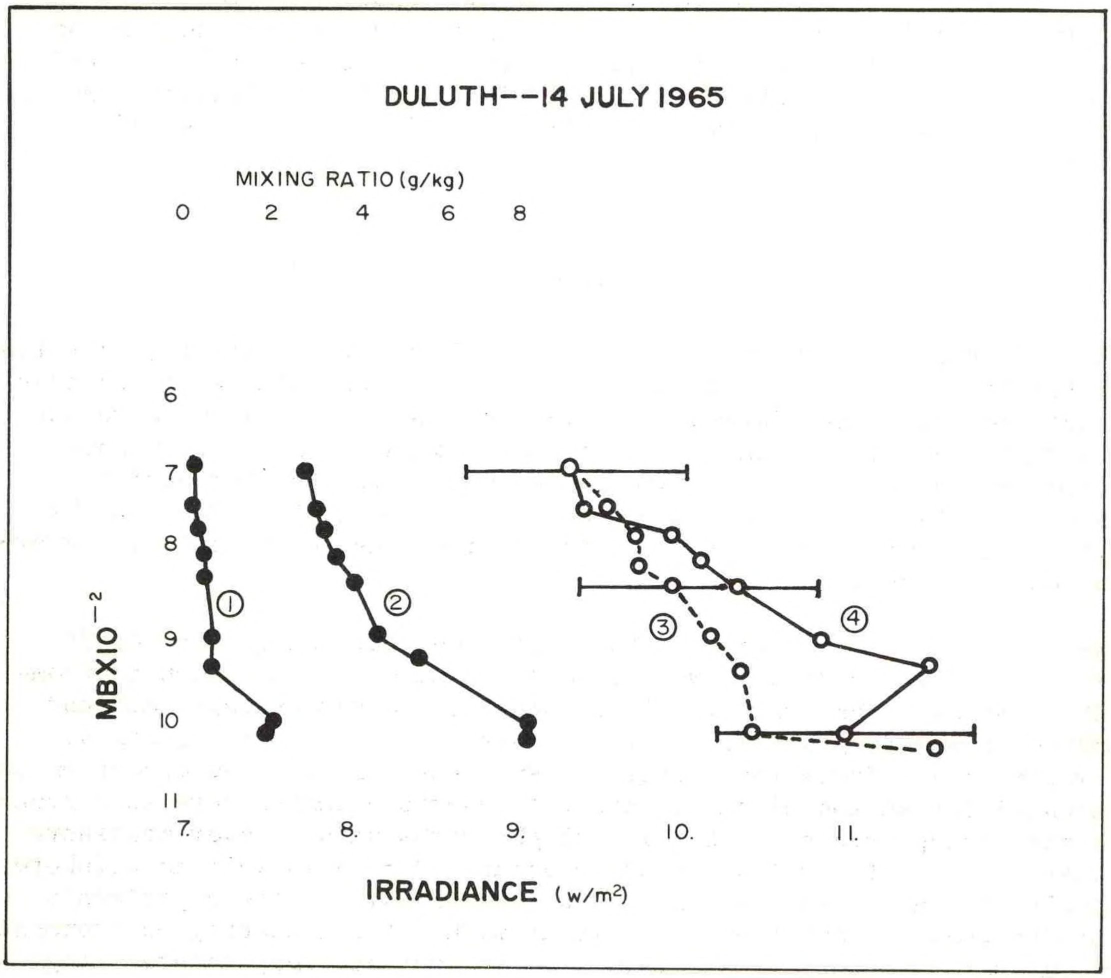

Figure 14.--Convergence of iterative transfer solution. Curves ①, ② and ③ are iterations coverging to the observed values shown as ④ .

demonstrate the feasibility of this technique for measurement of the water vapor profile.

The investigations previously considered in this section relate primarily to total atmospheric profiles for global scale meteorology. These studies have relatively few observations in the first 1,000 meters above the sea surface and not enough low level data points are included in the papers to satisfy our needs. Additional examples of these global, total atmospheric types of investigations are by Conrath (1969), Paulson (1967), Saunders (1967), Kuhn and McFadden (1967), Shaw (1966), and Davis and Viezee (1964).

SUMMARY

This literature search for specific equations for low-level (first 1,000 meters) temperature-humidity profiles above the sea surface has shown that in many cases the parameters investigated in the documented studies were not directly applicable to solving the problem of computing an environmental correction for radiation temperature measurements over the sea surface. Consequently, this effort shows that additional work must be done in the future to derive suitable low-level profile equations to fit existing over-water atmospheric data.

One approach would be an airborne experiment utilizing an aircraft equipped with a dropsonde and two radiometers (airborne radiation thermometers-ART) at different wave lengths. Sea surface temperature data and an atmospheric sounding profile would be obtained at specific locations over a water area. These wave-length measurements would be dependent on the environmental correction of the apparent sea-surface temperature as a function of the atmospheric profile. The flight paths should cover nearshore areas where the continental air mass is being modified as well as offshore in a completely marine environment (stable air mass). These experiments would be designed to derive an operational method for computing environmental corrections for radiometric measurement of sea-surface temperature using flight-level measurements of air temperature and humidity.

Another approach would be a detailed analysis of the ocean weather ship radiosonde soundings up to 1,000 meters above the sea surface. Together with the available ship sea surface data, this study would yield a number of different atmospheric profiles (temperature, humidity, etc.) at various oceanic locations and permit the derivation of models for temperature-humidity profiles that could be applied globally. This in turn could lead to deducing an improved ART environmental correction term.

ACKNOWLEDGMENTS

The author is indebted to the following individuals: V. E. Noble of the Airborne Remote Sensing Oceanography Project for reading the manuscript and giving invaluable comments; to R. J. Blake, U.S. Naval Oceanographic Office

Branch 2 Librarian, and R. Harmon, Naval Research Laboratory Reference Librarian, for their help in securing the background literature; M. M. Tyree for typing the final manuscript; and W. H. Lyons for the detailed illustrations.

REFERENCES

Bowne, N.E., and Clink, W.L., "A Survey of Temperature and Relative Humidity Fluctuations In the Lower Atmosphere," Final Report, The Travelers Research Center, Inc., Hartford, Conn., June 1966, pp. 1-107.

Bunker, A.F., Haurwitz, B., Malkus, J.S. and Stommel, H., "Vertical Distribution of Temperature and Humidity Over the Caribbean Sea," Papers In Physical Oceanography and Meteorology, Massachusetts Institute of Technology and Woods Hole Oceanographic Institution, Cambridge and Woods Hole, Mass., Vol. 11, No. 1, 1949, pp. 1-82.

Conrath, B.J., "On the Estimation of Relative Humidity Profiles from Medium-Resolution Infrared Spectra Obtained from a Satellite," Journal of Geophysical Research, Vol. 74, No. 13, June 20, 1969, pp. 3347-3361.

Craig, R.A., "Measurements of Temperature and Humidity In the Lowest 1,000 Feet of the Atmosphere Over Massachusetts Bay," Papers In Physical Oceanography and Meteorology, Massachusetts Institute of Technology and Woods Hole Oceanographic Institution, Cambridge and Woods Hole, Mass., Vol. 10, No. 1, 1946, pp. 1-47.

Craig, R.A., "Observations of Vertical Temperature and Humidity Distributions In the Convective Layer Above the Sea Surface," Annals of the New York Academy of Sciences, Vol. 48, 1947, pp. 783-788.

Craig, R.A., "Vertical Eddy Transfer Of Heat and Water Vapor In Stable Air," Journal of Meteorology, Vol. 6, No. 2, April 1949, pp. 123-133.

Craig, R.A., and Montgomery, R.B., "Evaporation (Measured) From the Ocean Into Hydrostatically Stable Air," Journal of Meteorology, Vol. 6, No. 6, December 1949, pp. 426, 427.

Davis, P.A., and Viezee, W., "A Model For Computing Infrared Transmission Through Atmospheric Water Vapor and Carbon Dioxide," Journal of Geophysical Research, Vol. 69, No. 18, September 15, 1964, pp. 3785-3794.

Emmons, G., "Vertical Distributions of Temperature and Humidity Over the Ocean Between Nantucket and New Jersey," Papers In Physical Oceanography and Meteorology, Massachusetts Institute of Technology and Woods Hole Oceanographic Institution, Cambridge and Woods Hole, Mass., Vol. 10, No. 3, 1947, pp. 1-89.

Fleagle, R.G., Deardorff, J.W., and Badgley, F.I., "Vertical Distribution of Wind Speed, Temperature, and Humidity Above A Water Surface," Journal of Marine Research, Vol. 17, 1958, pp. 141-155.

Gutnick, M., "Mean Annual Mid-Latitude Moisture Profiles to 31 Km," U.S. Air Force Office of Aerospace Research, Air Force Surveys in Geophysics, No. 147, AFCRL-62-681, July 1962, pp. 1-30.

Haltiner, G.P., and Martin, F.L., Dynamical and Physical Meteorology, McGraw-Hill Book Co., Inc., New York, N.Y., 1957, 470 pp.

Hasse, L., "On the Cooling of the Sea Surface By Evaporation and Heat Exchange," Tellus, Vol. 15, No. 4, 1963, pp. 363-366.

Holmboe, J., Forsythe, G.E., and Gustin, W., Dynamic Meteorology, John Wiley and Sons, Inc., New York, August 1957, 378 pp.

Hutcherson, D.C., "Water Vapor In the Atmosphere," Humidity and Moisture-Measurement and Control In Science and Industry, Vol. 2, Reinhold Publishing Corporation, New York, N.Y., 1965, pp. 486-494.

Kuhn, P.M., Ragotzkie, R.A., and Menon, V.K., "Double Bolometer Measurements of the Effects of Atmospheric Radiators," Technical Report No. 30, University of Wisconsin, Department of Meteorology, Madison, Wis., January 1967, 17 pp.

Kuhn, P.M. and McFadden, J.D., "Atmospheric Water Vapor Profiles Derived From Remote-Sensing Radiometer Measurements," Monthly Weather Review, Vol. 95, No. 8, Washington, D.C., August 1967, pp. 565-569.

Langer, R.M., Effects of Atmospheric Water Vapor On Near Infrared Transmission At Sea Level, J.R.M. Bege Company, Arlington, Mass., November 1958, 152 pp.

Lettau, H.H., and Davidson, B., Exploring the Atmosphere's First Mile, Vol. 1 and Vol. 2, Pergamon Press, New York, N.Y., 1957, 578 pp.

Montgomery, R.B., "Observations of Vertical Humidity Distribution Above the Ocean Surface and Their Relation to Evaporation," Papers In Physical Oceanography and Meteorology, Massachusetts Institute of Technology and Woods Hole Oceanographic Institution, Cambridge and Woods Hole, Mass., Vol. 7, No. 4, February 1940, pp. 1-30.

Montgomery, R.B., "The Taylor Diagram (Temperature Against Vapor Pressure) For Air Mixtures," Woods Hole Oceanographic Institution Collected Reprints--1950, August 1951, pp. 163-183.

Paulson, C.A., "Profiles of Wind Speed, Temperature and Humidity Over the Sea," Scientific Report, NSF GP-2418, October 1967, 128 pp.

Roll, H.U., Physics of the Marine Atmosphere, Academic Press, New York, N.Y., 1965, 426 pp.

Saunders, P.M., "Aerial Measurement of Sea Surface Temperature in the Infrared," Journal of Geophysical Research, Vol. 72, No. 16, August 15, 1967, pp. 4109-4117.

Saucier, W.J., Principles of Meteorological Analysis, The University of Chicago Press, Chicago, Ill., 1955, 438 pp.

Shaw, R.W., "Environmental Errors In the Use of the Airborne Radiation Thermometer," Thesis, University of Toronto, Ontario, Canada, April 1966, 58 pp.

Smithsonian Meteorological Tables, 6th Revised Edition, Smithsonian Institution, Washington, D.C., 1951, 527 pp.

Stephenson, S.T., "Some Measurements of Humidity, Temperature and Refractive Index Gradients Immediately Above the Ocean," Report WP-22, U.S. Navy Radio and Sound Laboratory, San Diego, Calif., September 1945, 14 pp.

Sutton, O.G., Micrometeorology--A Study of Physical Processes In the Lowest Layers of the Earth's Atmosphere, McGraw-Hill Book Co., Inc., New York, N.Y., 1953, 333 pp.

Sverdrup, H.U., "The Humidity Gradient Over the Sea Surface," Journal of Meteorology, Vol. 3, No. 3, March 1946, pp. 1-8.

Sverdrup, H.U., "Evaporation From the Oceans," Compendium of Meteorology, American Meteorological Society, Boston, Mass., 1951, pp. 1071-1081.

RELATED BIBLIOGRAPHY

Barnett, T.L., "Application of a Nonlinear Least-Squares Method to Atmospheric Temperature Sounding," Journal of Atmospheric Sciences, Vol. 26, No. 1, May 1969, pp. 457-461.

Bindon, H.H., "A Critical Review of Tables and Charts Used in Psychrometry," Humidity and Moisture--Measurement and Control in Science and Industry, Vol. 1, Reinhold Publishing Corporation, New York, N.Y., 1965, pp. 3-15.

Bunker, A.F., "On the Determination of Moisture Gradients from Radiosonde Records," Woods Hole Oceanographic Institution Collected Reprints--1953, Contribution No. 605, July 1954, pp. 406-409.

Craig, R.A., Katz, I., and Harney, P., "Sea Breeze Cross Sections from Psychrometric Measurements," Bulletin of the American Meteorological Society, Vol. 26, No. 10, December 1945, pp. 405-410.

Cramer, H.E., and Record, F.A., "The Variation of the Vertical Flux of Heat and Momentum," Journal of Meteorology, Vol. 10, No. 3, June 1953, pp. 219-226.

Gutnick, M., and Salmela, H.A., "Reevaluation of the Mid-latitude Moisture Profiles," Humidity and Moisture--Measurement and Control in Science and Industry, Vol. 2, Reinhold Publishing Corporation, New York, N.Y., 1965, pp. 495-501.

Hubert, W.E., "U.S. Fleet Numerical Weather Facility Activities Relating to Sea-Air Interactions on a Synoptic Scale," Proceedings of the U.S. Sea-Air Interaction Conference, Tallahassee, Florida, February 23-25, 1965, ESSA Technical Note 9-SAIL-1, pp. 239-256.

Hutcherson, D.C., "A Model Wet Atmosphere for Use in Infrared Range Calculations," Chance Vought Corporation AER-EOR 12907, June 1960, 15 pp.

Klevantsova, V.A., Bortkovskii, R.S., and Preobrazhenskii, L. Yu, "Methods of Gradient Measurement at Sea," Canadian Meteorological Branch, Meteorological Translations No. 14, 1968, pp. 55-67.

Kondrat'ev, K.YA., Niilisk, KH. YU., and Noorma, R. YU, "The Spectral Distribution of the Infrared Radiation in the Free Atmosphere," Izvestia, Atmospheric and Ocean Physics, Vol. 2, No. 2, 1966, pp. 121-136.

Kraus, E.B., and Morrison, R.E., "Local Interactions Between the Sea and the Air at Monthly and Annual Time Scales," Quarterly Journal of the Royal Meteorological Society, Vol. 92, No. 391, January 1966, pp. 114-127.

Mallow, R.D., "Atmospheric Water Vapor Transmission Coefficients for the Infrared Spectrum," Chance Vought Corporation No. 2-58000/3TM-1, April 2, 1963, 21 pp.

Mastenbrook, H.J., "Frost-point Hygrometer Measurements in the Stratosphere and the Problem of Moisture Contamination," Humidity and Moisture--Measurement and Control in Science and Industry, Vol. 2, Reinhold Publishing Corporation, New York, N.Y., 1965, pp. 480-485.

McAlister, E.D., "Infrared-optical Techniques Applied to Oceanography, 1, Measurement of Total Heat Flow from the Sea Surface," Applied Optics, Vol. 3, No. 5, May 1964, pp. 609-612.

McAlister, E.D., "A Two-wavelength Microwave Radiometer for Measurement of the Total Heat Exchange at the Air-Sea Interface," Applied Optics, Vol. 4, No. 1, January 1965, pp. 145-146.

McAlister, E.D., "Using Infrared to Measure Heat Flow from the Sea," Ocean Industry, Vol. 2, No. 5, May 1967, pp. 35-39.

McAlister, E.D., "Airborne Measurements of the Total Heat Flux from the Sea Surface: Progress Report," Fourth National ISA Marine Sciences Instrumentation Symposium, Vol. 4, Plenum Press, New York, N.Y., 1968, pp. 301-305.

Morrissey, E.G., "Ocean-Atmosphere Heat Exchange at Ocean Station Bravo," Canada --Department of Transport, Meteorological Branch, Toronto, Ontario, Circular 4301, Tec. 579, September 20, 1965, 11 pp.

Namias, J., "Seasonal Interactions Between the North Pacific Ocean and the Atmosphere During the 1960's" Monthly Weather Review, Vol. 97, No. 3, March 1969, pp. 173-192.

Roll, H.U., "On the Present State of Knowledge in Air-Sea Boundary Layer Problems," Proceedings of the U.S. Sea-Air Interaction Conference, Tallahassee, Florida, February 23-25, 1965, ESSA Technical Note 9-SAIL-1, pp. 31-63.

Ruskin, R.E., "Measurement of Atmospheric Dewpoint From Aircraft," Naval Research Laboratory Report 6725, June 12, 1968, 11 pp.

Schell, I.I., "On a Criterion of Representativeness of Sea Surface Temperature Data," Woods Hole Oceanographic Institution Collected Reprints--1959, Contribution No. 1029, November 1959, pp. 571-574.

Spar, J., "Air-Sea Exchange as a Factor in Synoptic-scale Meteorology in Middle Latitudes," Proceedings of the U.S. Sea-Air Interaction Conference, Tallahassee, Florida, February 23-25, 1965, ESSA Technical Note 9-SAIL-1, pp. 1-16.

Telegadas, K., and London, J., "A Physical Model of the Northern Hemisphere Troposphere For Winter and Summer," Scientific Report No. 1, New York University, College of Engineering Research Division, New York, N.Y., February 1954, 55 pp.